Solution-State Structure of Native Coenzyme F430 by NMR Methods

Hoshik Won*, Karl D. Olson**, Jisuk Park*, Ralph S. Wolfe**,
Dennis R. Hare***, and Michael F. Summers†

*Department of Chemistry, Hanyang University,

**Department of Microbiology, University of Illinois-Urbana Champaign, Urbana, IL 61801,

***Hare Research Inc., 14810 216th Ave. N.E., Woodinville, WA 98072 and

†Department of Chemistry and Biochemistry, University of Maryland Baltimore County, Baltimore, MD 21228

Received April 15, 1995

Solution-state structure of native F430 was determined by using NMR methods and NMR-based distance geometry (DG) computations. Structures were generated with loose NOE-derived interproton distance restraints (2.0-2.5 Å, 2.0-3.5 Å and 2.0-4.5 Å for strong, medium, and weak NOE cross-peak intensities, respectively). 2D NOESY back-calculations of structures were subsequently carried out for establishing the consistence between experimental data and DG-model structures. The back-calculated 2D NOESY spectra of resulting DG structures were well consistent with experimental 2D NOESY spectra. Superposition of 20 independent structures with macrocyclic ring atoms and all atoms of F430 afforded pairwise root mean square deviations (RMSD) of 0.025-0.125 Å and 0.64-1.3 Å, respectively. The macrocyclic rings of structures are well converged to a unique conformation with saddle-shaped deformation whereas most of side chains are not converged. The average dihedral angle (N1-N2-N3-N4, 27.78±1.50°) of 20 DG-structures exhibits that the macrocyclic ring conformation is puckered as much as 12,13-diepimeric F430 (28.75± 4.07°).

Introduction

Nickel(II)-containing coenzyme F430 is a non-fluorescent macrocyclic prosthetic group found in methanogenic bacteria.[1,2] Coenzyme F430 catalyzes the final step of methanogenesis by using two additional cofactors 2-methylthioethane sulfonic acid (Methyl CoM) and 7-mercapto-heptanoylthreonine phosphate (HS-HTP) as methane donor and reducing equivalent, respectively.[3,4] The conversion of CO_2 into CH_4 is believed to be an energy-yielding process in methanogens.

Structural features of F430 are essential for the understanding of F430-dependent functions and for the elucidating of its mechanistic pathway. Earlier structural studies of F430 were mostly made by X-ray crystallographic studies with a series of high-spin and low-spin Ni(II)-containing macrocyclic model complexes,[5,6] and by NMR studies[7,8] with a pentamethylester derivative of F430 (F430M). The first primary structure of F430 was non-crystallographically deduced from the NMR studies of F430M and extensive ^{13}C-labeled model complexes.[7] The absolute stereochemistry of C17 (see the chart I) could not be made due to severe signal overlap.[7,8] Recent NMR studies of native F430 provided the stereochemistries of C17-C18-C19 to be either R-R-S or S-S-R[9] and these stereochemistries were recently resolved by the X-ray crystallographic characterizations of 12,13-diepimeric F430M and solution-state structure determination of 12,13-diepimer F430.[10,11]

In addition to structural features, the coordination geometries and ligation modes of F430 were predicted on the basis of X-ray absorption spectroscopy (XAS) and extended X-ray absorption fine structure (EXAFS). For example, a four-coordination mode for 12,13-diepimeric F430 and a six-coordination for native F430 were predicted by comparing the X-ray absorption patterns of various Ni(II)-model complexes.[12,13]
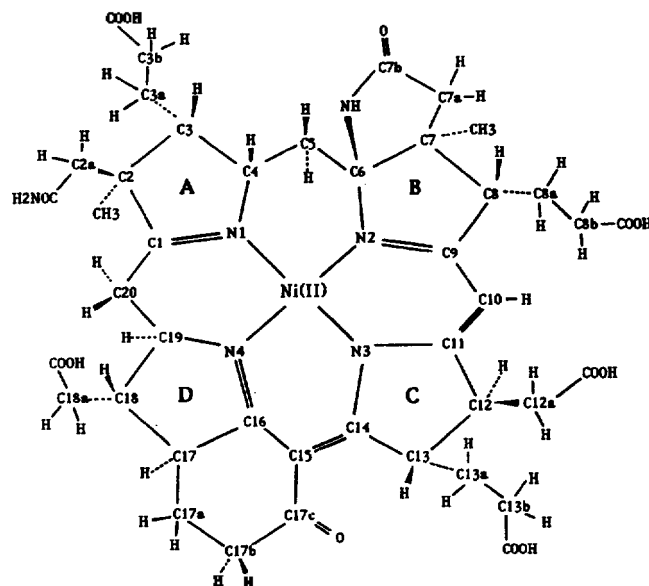
Although numerous spectroscopic characterizations of F430

Chart 1. Molecular structure of native coenzyme F430.

and its analogues were accomplished, the atomic-level structure of native F430 has not been obtained due to, in part, the difficulties in obtaining the suitable crystals for X-ray crystallographic studies. As an alternative way for the structure determination, a NMR-based solution-state structure determination was used in this study. Although the method employed in this study has been mostly utilized for large biopolymers,[14,15] a relatively new NMR-based DG method has successfully applied for the structure determination of relatively small molecule.[11] In addition, potential and limitaions of NMR approach were described. Application of NMR-based distance geometry (DG) and 2D NOESY back-calculations enabled the solution-state structure determination of native

650 *Bull. Korean Chem. Soc.* **1995**, Vol. 16, No. 7

Hoshik Won et al.

F430, and results were described here.

Experimental Section

Materials. Phenyl Sepharose CL-4B, QAE A-25 and DEAE-Sephadex A-25 were purchased from Pharmacia LKB Biotechnology Inc. C_{18} RP-HPLC (reverse phase high pressure liquid chromatography) columns were obtained from Waters. PM30 ultrafilteration membranes were purchased from Amicon. Deuterated trifluoroethanol (TFE-d_3) was purchased from Cambridge Isotopes. Bacterial cells were lab stock cultures.

Isolation of Native F430. Methanobacterium thermoautotrophicum strain ΔH, (DSM 1053) were grown in a 250 L fermenter (B. Braun) at 60 ℃, pH=7.3 with H_2 and CO_2 as carbon and energy sources, respectively. The medium was reduced with H_2S (to *ca.* 440 mV *vs.* NHE) before inoculation. During the fermenter running, H_2S, H_2 and CO_2 flow rates were adjusted manually and *via* computer to maintain a constant pH (0.15). As the cells reached the end of exponential growth (but before stationary phase) they were aerobically harvested (Sharples centrifuge). The cell paste was then immediately transfered into Wheaton bottles and made anaerobic by several nitrogen gas flushing cycles in an air lock of an anaerobic hood (Coy). The cells were stored under N_2 at −20 ℃ either as a cell paste or as a cell suspension of whole cells in 50 mM potassium phosphate (pH 7.0) buffer (1 : 1).

Native F430 was purified by utilizing hydrophobic interaction chromatography (Phenyl Sepharose) and anion exchange chromatography (QAE A-52 and DEAE A-52) as described previously.[9,12] Two additional HPLC systems were used for further purification of native F430. The eluent was monitored at both 560 nm and 430 nm using HPLC systems (I and II) : (HPLC SYSTEM I : Waters C_{18} μBondapak 3.9 mm×30 cm; 25 min linear gradient; 10% MeOH (50 mM NH_4CO_2H, pH 7.0) to 50% MeOH (50 mM NH_4CO_2H, pH 7.0); 0.5 mL/min); (HPLC SYSTEM II : Waters C_{18} μBondapak 7.8 mm×30 cm; 20 min linear gradient; 10% MeOH (50 mM NH_4CO_2H, pH 7.0) to 60% MeOH (50 mM NH_4CO_2H, pH 7.0); 1 mL/min.). Final purity of F430 was checked with UV/Vis spectrometric analyses and mass spectrometry, respectively. The characteristic absorbance ratio of A_{430}/A_{275} was 1.05, and fast atom bombardment (FAB) cation mass spectrum of native F430 gave a m/z value (=905). The elemental composition was determined to be $C_{42}H_{51}O_{13}N_6Ni$ by high resolution mass spectrometry.

NMR Data. NMR spectral data (500.14 MHz, ^1H) were obtained by using a GE GN-500 MHz spectrometer. Sample conditions were as follows : 5.1 mM native F430 in F_3CCD_2 OD (TFE-d_3) solvent; $T=20$ ℃. Raw NMR data were transfered *via* ethernet to Silicon Graphics Personal Iris computers, converted to "readable" files using an in-house program (GENET) and processed. ^1H chemical shifts were referenced to internal TFE (3.88 ppm, ^1H). NMR data processing, distance geometry calculations, and NOESY back-calculations were performed by using FTNMR, FELIX, DSPACE, and GNOE software packages. Data acquisition and processing parameters for individual 2D experiments were as below.

NOESY. NOESY experiments[16,17] were accomplished with following conditions; 2×256×1024 raw data matrix size; 64 scans per t_1 increment; 2.8 sec repetition delay period. Data for quantitative interproton distance analysis were acquired in TFE solutions with mixing times of 0.01, 0.05, 0.1, 0.3 and 0.5 sec. All NOESY data were processed with 6 Hz exponential line broadening in t_2, and 90°-shifted squared sine-bell filtering in t_1, with third-order polynomial baseline correction in the F_1 domain subsequent to the final Fourier transform.

ROESY. ROESY experiments[18,19] were accomplished with following conditions; 2×256×1024 raw data matrix× size; 64 scans per t_1 increment; 2.4 s repetition delay; 85 ms continuous wave spin lock period; 6.25 kHz spin lock field strength, corresponding to 40 μs 90° pulse widths; 6 Hz Gaussian and 90°-shifted squared sine-bell filtering in the t_2 and t_1 domains, respectively.

Primary and Experimental NOE Restraints

Primary distance restraints, including covalent connectivities and molecular planarity dictated by electronic conjugation, were obtained from previous X-ray crystallographic results of relevant molecules.[20,21] Restraints were included to enforce planarity for several conjugated atoms : N2, C9, C10, C11, C14, C15, C16, N3, N4, C17c and OC17c. Planarity restraints were simply obtained by using the geometric identity of internal coordinates. Moderate restraints were also included to enforce planarity of the exocyclic lactam moiety. Side chain amide groups and five carboxyl groups were constrained to minimize van der Waals repulsion with methylenyl protons on the neighboring carbons. The van der Waals radii of atoms were employed as follows : H, 0.95 Å, C, 1.5 Å, N, 1.3 Å, O, 1.3 Å, Ni, 0.7 Å.[22] The primary structure dictated the close approach of several atoms to distances smaller than their standard van der Waals radii, including the C17c carbonyl oxygen to atoms associated with C13 and the close approach atoms on the fused lactam moiety.

Planarity restraints of the six-membered ring associated with C14-C15-C16-C17c-N4 ring conjugation were set to as follow : C14-OC17c (2.67- infinite Å), C13-OC17c (2.3-2.5 Å), H13-OC17c (1.5-infinite Å), C13a-OC17c (1.5-infinite Å), C17c-C13 (2.7-3.1 Å). In six-membered ring, atom pairs were allowed to approach to distances smaller than the sums of their van der Waals radii. For example, standard radii for carbons of the six-membered ring necessarily led to a flattening of the ring due to the van der Waals repulsion terms. As such, carbon pairs of the six-membered ring separated by three bonds were allowed to approach to 2.85 Å (determined as the minimum separation observed in X-ray structures of several sugars and steroids), which enabled the maximum sugar pucker observed from the X-ray crystallographic studies of relevant sugar and steroid structures.[23] All planarity restraints used to allow sub-van der Waals approach of atoms are follow : C15-C17a (2.85-3.91 Å), C16-C17b (2.85-3.92 Å), C17-C17c (2.85-3.90 Å).

The distance restraint of Ni-N bond was set to 2.0-2.05 Å by averaging various Ni(II)-containing macrocyclic model complexes.[6,24] Bond distance of Ni-N has been reported for native F430 and 12,13-diepimeric F430 (or F430M). For example, the Ni-N bond distance of 12,13-diepimeric F430 (1.89

Table 1. NOE Restraints of Native F430 Used for Structure Determination*

H3 restraints	(unit/Å)	H18 restraints	(unit/Å)
H3-H3br	2.0-3.5	H18-H18ar	2.0-3.5
H4 restraints		H19 restraints	
H4-H3	2.0-2.5	H19-H20s	2.0-2.5
H4-H3br	2.0-4.5	19-H17	2.0-3.5
H4-H5r	2.0-2.5	Me2 restraints	
H8 restraints		Me2-H20r	2.0-3.5
H8-H8ar	2.0-2.5	Me2-H2ar	2.0-3.5
H8-H8as	2.0-3.5	Me2-H2as	2.0-3.5
H8-H8br	2.0-3.5	Me2-H3ar	2.0-3.5
H10 restraints		Me2-H3as	2.0-3.5
H10-H12	2.0-3.5	Me2-H5s	2.0-3.5
H10-H8	2.0-3.5	Me7 restraints	
H10-H12ar	2.0-3.5	Me7-H7as	2.0-3.5
H12 restraints		Me7-H5s	2.0-3.5
H12-H12as	2.0-3.5	Me7-H5r	2.0-3.5
H12-H13br	2.0-3.5	Me7-H8ar	2.0-2.5
H12-H13bs	2.0-3.5	Me7-H8bs	2.0-4.5
		Me7-H8	2.0-4.5

*r, s refer to prochiral R and S assignments obtained from the results of DG and 2D-NOESY back-calculations.

Å) and native F430 (2.1 Å) was obtained from the EXAFS-derived Ni-N,O distance observations.[12,13] The Ni-N bond length (relatively short *ca.* 1.85 Å) was found in the 12,13-diepimeric F430M.[10]

NOE-derived distance restraints were obtained *via* qualitative assessment of NOE cross peak volumes in the NOESY spectra. For many protons, direct dipolar cross relaxation could be distinguished from spin diffusion on the basis of the 2D ROESY spectrum. However, no restraints were included to attempt to fit the spin diffusion cross peaks. Instead, loose NOE restraints were used for cross-peaks classified as strong, medium, and weak. The ranges of initial NOE restraint were assigned with 2.0-2.5 Å (strong cross peak intensities), 2.0-3.5 Å (medium cross peak intensities) and 2.0-4.5 Å (weak cross peak intensities) in Table 1.

Structure Generation and Refinement

NMR-based DG structures were generated with the program DSPACE and structures embeded in 3-dimensional space with the metric matrix method are subjected to simulated annealing (SA) and conjugated gradient minimization (CGM). The embedded initial coordinates containing violations of the upper and lower boundary restraints were then refined by using trial distances generated by selecting random distances between the upper and lower bounds of each element. Complete refinements were achieved with additional algorithm that adds a random vector of user-specified magnitude (0.2-0.3 Å) to the coordinates of each atom in order to randomize the structure and with a subsequent SA algorithm. After minimization to a moderate target penalty (*ca.* 0.3 Å²), the initial DG structure was saved and new DG structures were generated by performing two 10 Å randomizaitons of atom positions, followed by SA and CGM refine-

ment. Once a low-penalty (penalty=squared sum of the covalent and experimental bounds violation) structure was stored, new starting coordinates were then obtained by performing different embeding, SA, CGM algorithms. Further refinement was achieved by application of variable velocity simulated annealing (to maximum penalty values of 10-20 Å²), SHAKE (to penalties of *ca.* 10 Å²) and CGM algorithms.

A set of DG structures which included NOE-derived distance restraints were generated (DG-NOE). Prior to further refinements, initial DG-NOE structures exhibited penalty values in the range of 0.03-0.3 Å². Final DG-NOE structures followed by SA, SHAKE, CGM refinements with variable velocity and penalty values exhibited penalty values in the range 0.03-0.08 Å². The detailed procedures used for DG-structure generation and refinement are the same as that of the structure determination of 12,13-diepimeric F430.[11]

The complete time course for nuclear relaxation was then determined for each refined structure *via* numerical integration of the Bloch equations. As described previously,[14] this approach accurately accounts for spin diffusion. Z-leakage rate constant K_{zL}, accounting for the loss of Z-magnetization within mixing period, was used with 1 sec^{-1} (3 sec^{-1} for Me2 and Me7). A cross relaxation rate constant K_σ which governs the cross relaxation rate was used with 60 sec in this NOE back-calculation. K_σ was determined by using NOE build-up curve comparisons in advance with well resolved geminal protons (H5, H5') which is structurally known internuclear distances with 1.8 Å.

2D-NOESY back-calculations give a list of normalized auto- and cross-peak intensities for selected increasing mixing times. Profiles of these outputs provide the theoretical NOE build-up curves. The results of back-calculation were then assigned to GNOE in order to generate the theoretical 2D NOEs. A consecutive serial files, obtained from GNOE calculations for different mixing times, were incorporated into FTNMR/FELIX to generate 2D NOE back-calculated spectra which could be directly compared with the experimental spectra. Consistencies between experimental and back-calculated NOESY spectra were used as a major criteria for evaluating the suitability of the DG structures. The back-calculated 2D NOE spectra of DG-NOE(8) (lowest penalty value, 0.032 Å²) are consistent with the experimental NOE spectra in Figure 1. Even with loose NOE restraints, the NOE behaviors of back-calculated spectra associated with H10, H4, H19 and Me2 (methyl group on C2) are well agreed with experimental NOEs. After the spectral comparisons, the resulting trial curves of DG-NOE(8) were compared with experimental NOE build-up profiles.

Results and Discussion

A relatively new NMR-based distance geometry (DG) approach has enabled the three-dimensional structure determination of native coenzyme F430. The randomly oriented two side chains (C12, C13) were observed due to insufficient NOE restraints, including labile H13 proton and NMR signal overlap of H12ar, s geminal protons. As a result of structure determination, all NOEs of the geminal protons that were earlier assigned to be up (prime) and down field now reassigned with *prochiral R, S* definition which shows stereospecific orientation of F430 (see Table 2).[9] For instance, experi-
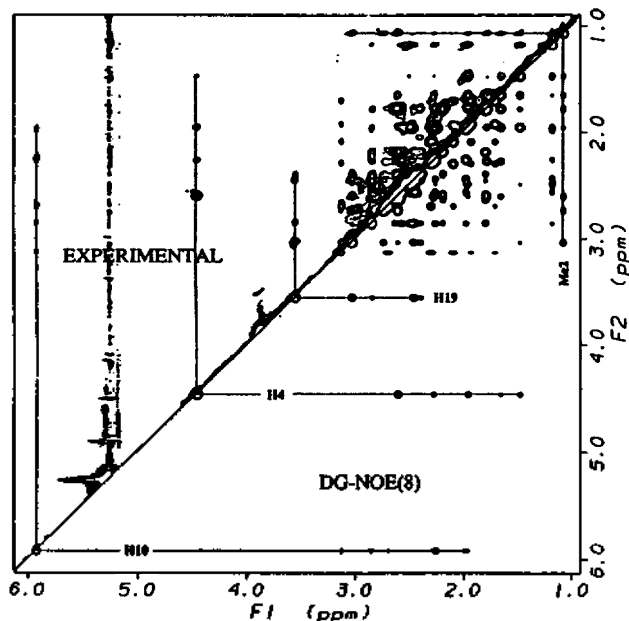
Figure 1. Experimental and back-calculated 2D NOE spectra of DG-NOE(8) structure at 300 ms mixing period. Several of consistencies between experimental and back-calculated spectra are labeled for four protons H10, H4, H19 and Me2.
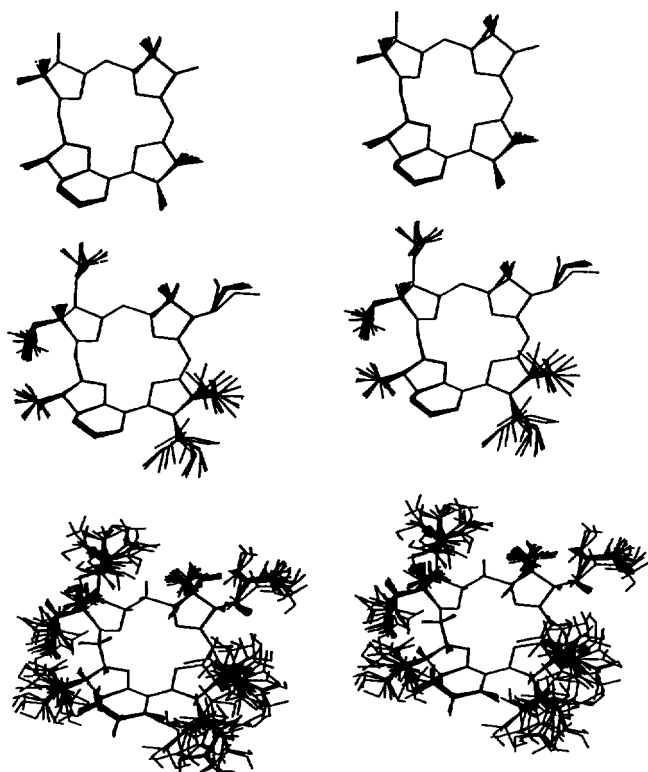

Figure 2. Superposition of 20 independent DG structures generated with loose NOE restraints. Superpositions were made for the macrocyclic ring atoms only (top), all atoms except hydrogens (middle) and all atoms (bottom).

mental and back-calculated NOE buildups for signals associated with Me2, H4 and H3 protons results in proper stereochemistry of geminal protons attached to C2a, C3a and

Table 2. Prochiral Assignments and NOESY of Native Coenzyme F430*

Signal	Chemical shifts	NOESY
Me2	1.08	H2as(s); H2ar(s); H3(relay, overlap with H2as) (s); H3ar(w); H3as(w); H3br,s(w); H5s(s); H5r (w); H20r,s(s)
Me7	1.18	H5s(s); H5r(s); H7ar,s(s); H3br,s(s); H8(w); H8 bs(s); H8br(s); H8as(overlaps with H5r signal) (s); H8ar(s)
H2as	2.60	H2ar(s); Me2(s)
H2ar	2.73	H2as(s); Me2(s); H18ar,s(w)
H3	2.60	Me2(s); H3ar(m); H3as(m); H4(s); H3br,s(s); H5r(m)
H3ar	1.65	H5s(w); Me2(m)
H3as	1.77	Me2(m); H3ar(s); H5s(w);
H3br,s	2.26	H3ar(m); H3as(m); H5s(w); H5r(s);
H4	4.45	H3(s); H3br,s(w); H5s(w); H5r(w)
H5s	1.48	Me2(m); Me7(s)
H5r	1.95	Me2(m); Me7(s); H3as(m); H3ar(m); H5s(s)
H7ar,s	2.49	H5s(w); H5r(m); Me7(s); H8as(w); H8ar(w)
H8	2.86	H7ar,s(s); H8as(m); H8ar(m); H8bs(s); H8br (w); Me7(w);
H8as	1.98	H5s(s); H10(m); Me7(s)
H8ar	2.26	Me7(s); H8as(s); H8as(w); H8ar(m)
H8bs	2.44	H8br(s); H8as(w); H8ar(m)
H8br	2.56	H8bs(s); H8as(w); H8ar(m)
H10	5.91	H8(m); H8as(m); H8ar(s); H12(m); H12ar,s(m)
H12	3.13	H12ar,s(s); H13ar(w); H13as(w); H13bs(w); H 13br(w)
H12ar,s	2.67	H12(s)
H13	3.91	None
H13ar	1.71	H13ar(s); H13br(w); H13bs(w)
H13as	1.93	H13as(s); H13br(w); H13bs(w)
H13bs	2.09	H13br(s); H13ar(w); H13as(w)
H13br	2.29	H13bs(s); H13ar(w); H13as(w)
H17	2.83	H17as(w); H17ar(m); H17bs(m); H17br(m); H 18(m); H18ar,s(s)
H17as	1.78	H17ar(s)
H17ar	2.19	H17as(s)
H17bs	2.58	H17as(s); H17ar(s); H18ar,s(w)
H17br	2.63	H17as(s); H17ar(s); H18ar,s(w)
H18	2.38	H17as(m); H17ar(m)
H18ar,s	2.45	H17as(m); H17ar(m)
H19	3.55	H17(m); H18(m); H18ar,s(s); H20r,s(s)
H20r,s	3.02	Me2(s); H2ar(s); H17(relay,w); H18(s); H18ar,s (s); H2as(s)

*s, m, and w refer to strong, medium, and weak NOESY cross peak intensities, respectively.

C5 carbons. Except for overlapping geminal protons on C3b, C7a, C8b, C12a and C18b carbons, prochiral assignments were made for all geminal protons. Because of insufficient NOE information on C-ring side chains, tentative prochiral assignments were made for two geminal protons of the C13 side chain on the basis of relative NOE intensities from H12

proton.

The degree of convergence provides an assessment of the ability of the distance data to define a single conformation. Convergence was assessed by superposition of macrocyclic atoms N1, C5, N2, C10, N3, C15, N4, C20. The superposition of DG-NOE(1-20) structures gave well-converged conformation except for several side chains (C3a, C12a, C13a, and C18a) that could not be restrained with NOE restraints due to severe signal overlaps as shown in Figure 2. The resulting macrocyclic ring from this DG method has a saddle-shaped structure. The ring conjugation of the N2, C9, C10, C14, C15, C16, C17c and N4 atoms made the molecular structure be relatively planar. However, the averaged dihedral angle (N1-N2-N3-N4, 27.78± 1.50°) of 20 DG-NOE structures shows that the macrocyclic ring is puckered as much as 12,13-diepimeric F430 (28.75± 4.07°). For DG-NOE structures, the superpositions of macrocyclic ring atoms and all atoms gave RMS deviation values in the range of 0.025 to 0.125 Å and 0.64 to 1.3 Å, respectively. The major structural differences between native F430 and 12,13-diepimeric F430 were observed to be structural variation associated with six-membered ring, whereas two isomers have similar puckering angles in terms of N1-N2-N3-N4 dihedral angle. The conformations of the A-, B-, C- and D-ring are Me2(axial)-H3(axial)-H4 (equatorial), Me7(axial)-H8(axial), H12(equatorial)-H13(equatorial), and H17(axial)-H18(axial)-H19(axial), respectively, for all of 20 DG-NOE structures. As identified in the structure determination of 12,13-diepimeric F430, 2D NOE back-calculations played an important role in identifying specific orientation, prochiral assignments and good convergence of DG structures, but were not inevitable for good convergence of DG structures.

References

1. (a) Gunsalus, R. P.; Wolfe, R. S. *FEMS Micro. Lett.* **1978**, *3*, 191. (b) Gunsalus, R. P.; Romesser, J. A.; Wolfe, R. S. *Biochemistry* **1978**, *17*, 2374.
2. Diekert, G.; Konheiser, U.; Piechulla, K.; Thauer, R. K. *J. Bacteriol.* **1981**, *148*, 459.
3. Walsh, C. T.; Orme-Johnson, W. H. *Biochemistry* **1987**, *26*, 4901.
4. Rouviere, P. E.; Wolfe, R. S. *J. Biol. Chem.* **1988**, *263*, 7913.
5. Fässler, A.; Pfaltz, A.; Müller, P. M.; Farooq, S.; Kratky, C.; Kr utler, B.; Eschenmoser, A. *Helv. Chim. Acta.* **1982**, *65*, 812.
6. Kratky, C.; Fässler, A.; Pfaltz, A.; Kräutler, B.; Jaun, B.; Eschenmoser, A. *J. Chem. Soc., Chem. Comm.* **1984**, 1368.
7. Pfaltz, A.; Juan, A.; Fässler, A.; Eschenmoser, A.; Jaenchen, T.; Gilles, H. H.; Diekert, G.; Thauer, R. K. *Helv. Chim. Acta.* **1982**, *65*, 828.
8. Pfaltz, A.; Livingston, D. A.; Juan, B.; Diekert, G.; Thauer, R. K.; Eschenmoser, A. *Helv. Chim. Acta.* **1985**, *68*, 1338.
9. Won, H.; Olson, K. D.; Wolfe, R. S.; Summers, M. F. *J. Am. Chem. Soc.* **1990**, *112*, 2178.
10. Färber, G.; Keller, W.; Kratky, C.; Jaun, B.; Pfaltz, A.; Spinner, C.; Eschenmoser, A. *Helv. Chim. Acta* **1991**, *74*, 697.
11. Won, H.; Olson, K. D.; Hare, D. R.; Wolfe, R. S.; Kratky, C.; Summers, M. F. *J. Am. Chem. Soc.* **1992**, *114*, 6880.
12. Shiemke, A. K.; Kaplan, W. A.; Hamilton, C. L.; Shelnutt, J. A.; Scott, R. A. *J. Biol. Chem.* **1989**, *264*, 7276.
13. Shiemke, A. K.; Shelnutt, J. A.; Scott, R. A. *J. Biol. Chem.* **1989**, *264*, 11236.
14. Summers, M. F.; South, T. L.; Kim, B.; Hare, D. R. *Biochemistry* **1990**, *29*, 329.
15. Clore, G. M.; Gronenborn, A. M. *Science* **1991**, *252*, 1390.
16. Jeener, J.; Meier, B. H.; Bachmann, P.; Ernst, R. R. *J. Chem. Phys.* **1979**, *71*, 4546.
17. Macura, S.; Ernst, R. R. *Mol. Phys.* **1980**, *41*, 95.
18. Bax, A. *J. Magn. Reson.* **1988**, *77*, 134.
19. Rance, M.; *J. Mag. Reson.* **1987**, *74*, 557.
20. Rossi, M.; Glusker, J. P.; Randaccio, L.; Summers, M. F.; Toscano, P. J.; Marzilli, L. G. *J. Am. Chem. Soc.* **1985**, *107*, 1729.
21. Hodgkin, D. C.; Pickworth, J.; Robertson, J. H.; Prosen, R. J.; Sparks, R. A.; Trueblood, K. N. *Proc. R. Soc. London* **1959**, *A251*, 306.
22. Blake, P.; Hare, D. R.; Summers, M. F. in *Techniques in Protein Chemistry II*; Academic Press: 1990; p 357-368
23. Wheatley, P. J. *Physical Methods in Hetrocyclic Chemistry*; 2nd ed.; Academic Press: 1972; p 520, 492, 479.
24. Waditschatka, R.; Kratky, C.; Jaun, B.; Heinzer, J.; Eschenmoser, A. *J. Chem. Soc. Chem. Comm.* **1985**, 1604.